



## Research Article

# A novel WC–W<sub>2</sub>C composite synthesis by arc plasma melt cast technique: microstructural and mechanical studies



N. Nayak<sup>1</sup> · T. Dash<sup>1</sup> · D. Debasish<sup>2</sup> · B. B. Palei<sup>2</sup> · T. K. Rout<sup>3</sup> · S. Bajpai<sup>2</sup> · B. B. Nayak<sup>2</sup>

Received: 5 August 2020 / Accepted: 28 December 2020 / Published online: 26 February 2021

© The Author(s) 2021 [OPEN](#)

## Abstract

WC–W<sub>2</sub>C composites of three different compositions have been synthesized from mixture of WC + W (0, 5 and 16 wt% W) by thermal arc plasma melt-cast technique. Various grown phases observed in the composites consisting of major phases of WC and W<sub>2</sub>C and minor phases of unbound C (graphite) and tungsten (W) were confirmed by X-ray diffraction, selected area electron diffraction, X-ray photoelectron spectroscopy and Fourier transform infrared studies. Transmission electron microscopy and field emission scanning electron microscopy show polycrystalline nature of composites. Energy dispersive spectroscopy (of X-ray) infers the absence of any impurity in the composite. Almost porous free nature of composites were observed from X-ray micro computed tomography and BET analysis studies. WC–W<sub>2</sub>C composite (16 wt% W) shows 25% and 21% higher micro hardness (2535 VHN) and Young's modulus (625 GPa) values than that of pure melt cast WC sample.

**Keywords** Thermal arc plasma · Tungsten carbide · X-ray photoelectron spectroscopy · X-ray micro computed tomography · Microstructure · Microhardness

## 1 Introduction

Tungsten carbide generally occurs in two phases, viz. WC and W<sub>2</sub>C. While some literature report higher hardness for WC, the recent ones mention higher hardness for W<sub>2</sub>C [1–4]. For industrial practice fused tungsten carbide- a composite of WC and W<sub>2</sub>C is produced by melting and followed by cooling of up to room temperature. W–C Phase diagram indicates a pseudo-eutectic point at 2530 °C which follows eutectoid decomposition below 2380 °C to form a mixture of WC and W<sub>2</sub>C (Fig. 1) [5, 6]. The authors have taken advantage of such a decomposition to prepare WC–W<sub>2</sub>C composite at three different compositions by arc plasma melt casting of W and WC pellets prepared from their powder mixture mixed at different proportions. The mono carbide of tungsten (WC) characterized with

superior properties like high melting point (2750 °C) and high hardness (16–22 GPa) [7–9]. Kim and co-workers [10] reported hardness of binderless WC to be 2486 VHN with 97.6 relative density (%). When 10 wt% Co is added to WC (relative density—98.9%) the fracture toughness increases from 6.6 to 11.6 MPa m<sup>1/2</sup> in expense of decrease in hardness from 2486 to 1756 VHN. Similar kind of result was also obtained by Almond et al. [11] for WC-10 wt% Co sample showing hardness of 1333 VHN. Hence though metallic binder increases toughness but it hampers hardness behaviour of tungsten carbide ceramic. Hence to meet industrial requirement, it is required to prepare binder less WC–W<sub>2</sub>C composite with improved microstructural and mechanical properties. But there are few challenges associated in developing binderless WC–W<sub>2</sub>C composite for fully densifying the sintered body together

✉ T. Dash, tapan.dash@cutm.ac.in | <sup>1</sup>Centurion University of Technology and Management, Bhubaneswar, Odisha, India. <sup>2</sup>CSIR-Institute of Minerals and Materials Technology, Bhubaneswar, Odisha, India. <sup>3</sup>Research and Development Department, Tata Steel Ltd, Duburi, Odisha, India.



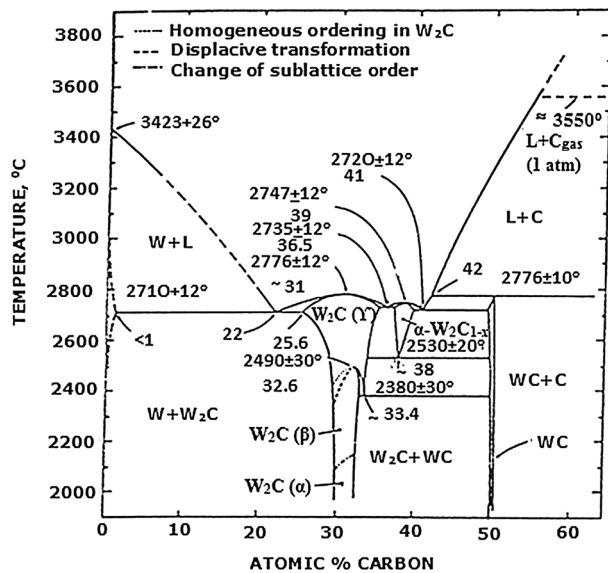


Fig. 1 W–C phase diagram [Ref 5, 6]

for achieving a high hardness and toughness composite. Tungsten carbide used in producing critical components such as spray injection nozzle, sand blasting nozzle, guide sleeve in machines, micrometre anvil, centre for lathe and grinder, rock cutting drill bit, etc. [12–18]. Applications of tungsten carbide metal matrix composites are found in the mining industry to coat different drilling and digging parts, in agriculture for coating on plough shares, tillage equipment and cutters. In steel industry tungsten carbide coatings used for example for guide rollers. Oil industry also uses this type of coatings in high wear applications. It is expected that the productivity of mining operations can be increased by 15% by using the nanocrystalline cemented tungsten carbide materials that increases tool life and reduces down time. The nanocrystalline cemented tungsten can also be used for metal working cutting tool to increase productivity. In rock cutting and hard facing applications, it is widely observed that WC–W<sub>2</sub>C composite shows better performance than pure WC [12]. WC–W<sub>2</sub>C composite shows better metal and stone cutting performance than pure WC. Since shielding behaviour of solid towards neutron demands reduced porosity, a WC–W<sub>2</sub>C composite with minimum porosity is required for *tokamak* application because of having high neutron absorption coefficient [19].

It is challenging to prepare WC–W<sub>2</sub>C composite without any addition of metallic binder because it involves high temperature. Generally powder metallurgy process and melt-casting processes employed to fabricate tungsten carbide and its products. Samples prepared by powder metallurgy process uses a number of steps such as binder mixing, compaction and sintering of samples etc. But samples

prepared by melt-casting of tungsten carbide into desired shape and size are less cumbersome and relatively easy to practice in industrial production. Melt-cast components also exhibit lower porosity compared to sintered ones. Because of high melting point of tungsten carbide, generally induction furnace and graphite furnace are employed in industries to melt this compound [20, 21]. But both the heating processes are generally costly and energy expensive. Thermal arc plasma (transferred arc mode) technique is an alternative to induction and graphite furnaces due to many advantages in melting high temperature products [12, 22–25]. Therefore it is chosen for preparation of melt casting of tungsten carbide.

WC–W<sub>2</sub>C composites of three different compositions (0, 5 and 16 wt% W) have been prepared by arc plasma melt-cast technique and their microstructural and microhardness properties have been studied using “X-ray diffraction (XRD), transmission electron microscopy (TEM), field emission scanning electron microscopy (FESEM), optical microscopy, energy dispersive spectra (EDS) of X-ray, selected area electron diffraction (SAED), fourier transform infra-red (FTIR), X-ray micro computed tomography (CT), X-ray photoelectron spectroscopy (XPS), BET (Brunauer–Emmett–Teller) analysis, micro hardness and Young’s modulus measurements”. This research work shows significant improvements in microhardness and Young’s modulus values for WC–W<sub>2</sub>C composite (WC + W (16 wt%)) than that of pure melt cast WC sample. Density analysis of composites was determined fifteen times for each composite following Archimedes’ principle by weighting the composites in the air as well as after dipping in 100 °C distilled water for 4 h.

## 2 Materials and synthesis

### 2.1 Arc plasma melt-cast of composite

WC and W were mixed at three different ratios as follows; WC: 100, 95, 84 wt% and W: 0, 5, 16 wt% to prepare respective homogeneous mixtures. The specifications of the used powder are as follows: W powder- grain size 5–6 μm and WC powder- grain size 5–8 μm. The chemical composition analysis of starting WC powder is shown in Table 1. The C % in starting WC powder is about 6 wt%. When W (0–15 wt%) added in WC, the wt% of C was varied. WC + W (5 wt%) composition contains theoretically W% and C% as 94.16 wt% and 5.84 wt% respectively. Similarly WC + W (16 wt%) composition contains theoretically W% and C% as 94.86 wt% and 5.14 wt% respectively. The homogeneous mixture samples of WC + W were prepared by using a dual drive dry planetary ball mill. The homogeneous mixture samples prepared by 5 h of ball milling. Argon atmosphere in the

**Table 1** The Chemical composition analysis of starting WC as follows

Element/Compound	% of present
WC	99.8
Total C	6.14–6.17
Free C	0.05
O	0.04
Fe	0.014
Cu	0.0002
Cr	0.004

mill was maintained to avoid oxide phase formation in the composite. The ball mill has two cylindrical jars and gyratory shaft. By the help of attached motor the shaft and two jars were rotated at 300 and 150 rpm respectively. In the two jars samples to ball ratio 1:10 were maintained during ball milling. The tungsten carbide balls of ratio 6 (8 mm dia.):4 (4 mm dia.) were used in the ball milling. The shearing and impact energy developed inside the jars used for producing homogenous and fine particles of tungsten carbide composite.

Samples were prepared at 0.1 kg scale. The above compositions were considered by following the phase diagram presented in Fig. 1. Pellets of tungsten monocarbide (WC) and tungsten (W) powder samples were prepared using poly vinyl alcohol (PVA) binder and by applying 6 T load for 30 s. Melt-casting of pellets were carried out in a 30 kW (dc) extended arc type plasma reactor using graphite crucible. Ar was employed as plasmagen gas and in situ melt casting of composites was carried out. Arc plasma melting was carried out in a 30 kW extended arc plasma furnace at current: 300–350 A and voltage: 45–60 V. Before plasma melting of samples carried out, preheating of plasma chamber was carried out at current: 100 A and voltage: 40 V for 5 min for removing unwanted contaminates. Around 3000 °C temperature was maintained during the melting of pellets. Plasma forming gas argon (Ar) was introduced into the reactor through an axial hole in the graphite cathode (top electrode) at a rate of 2 L per min. Sample was kept in crucible served as anode. Plasma was initiated by bringing cathode to very close to anode. Then stable arc length (2 cm) was maintained between cathode and anode. It took 10–15 min to completely melt the charge in the crucible. Then, the liquid melt was solidified for casting for 4–5 h within the graphite crucible by switching off power and allowed for cooling in the furnace.

## 2.2 Apparatus used for characterization of composites

X-ray diffraction (XRD) was taken by PANalytical X'Pert Pro diffractometer (CuK $\alpha$ ,  $\lambda = 0.15406$  nm). The microstructures

were observed by optical and transmission electron microscopy (TEM): TECNAI G<sup>2</sup> (200 kV), FEI, Netherland. Elemental compositions were studied by energy dispersive X-ray spectroscopy (EDS) attached to TEM. SAED analysis of composite was done with facility available with TEM. Fourier transform infra-red (FTIR) spectra were measured in the range of 400–4000 cm<sup>-1</sup> (Spectrum GX, Perkin Elmer). The pore volume was determined by BET method (ASAP 2020). Microhardness and Young's modulus was determined by UMIS system (Fisher-Cripps, Australia) with diamond Berkovich indenter. Density of samples was determined by following Archimedes' principle. Binding energy (B.E.) of elements were determined by X-ray photoelectron spectroscopy (XPS) analysis by using model S/N:1000:1, Prevac, Poland.

Internal and external (surface) imaging and microstructural investigation was performed by an X-ray micro computed tomography (model: SkyScan 2211, Bruker, Belgium). Reconstruction of scanned images was performed by using SkyScan's InstaRecon software. Sample was scanned with a full 3600 rotation (0.20 increments) at following conditions: accelerating voltage—185 kV and target current- 230  $\mu$ A. The reconstructed images were transferred into 3D models using CT vox and Avizo 9.0.0 platforms.

## 3 Results and discussion

### 3.1 Composites preparation by plasma treatment method

The melt-cast composites were prepared for three different compositions at the following range: W 0–16 wt%, WC 100–84 wt%. Product yield varied between 85 and 90% after plasma treatment. Power consumption recorded between 11.0 and 16.4 kWh per 0.1 kg during melt-cast process. Plasma experiment carried out under inert atmosphere (Ar) to avoid any chance of oxidation in the composite. Experiments conditions adopted for melt casting of WC + W (0–16 wt) samples presented in Table 2. The samples were produced in solid form after melt-cast treatment. Then for some characterizations like FESEM, micro CT, XPS, EDS and microhardness solid samples were mirror polished and powder samples were prepared for XRD FTIR, TEM and BET analyses.

### 3.2 XRD study

XRD analysis was carried out (Fig. 2) to identify different phases and planes grown in the composites. Phases grown in the melt cast composites were detected from their XRD results by comparing the observed *d* spacing

**Table 2** Experimental conditions adopted for melt casting of WC+W (0–16 wt%) samples and evaluation of pore volume, density and microhardness properties

Sample ID	Wt% in the mixture of compositions				Electrical energy consumed (kWh/0.1 kg)	Pore volume determined by BET method (cm <sup>3</sup> /g)	Density (g/cm <sup>3</sup> ) determination of composites by Archimedes' principle	Microhardness (VHN)	Young's modulus (GPa)
	W	WC	C (calc. theor.)	W (calc. theor.)					
Pure WC	0	100	6.13	93.87	11.0	0.005	16.5	2020 ± 10	510
WC+W 5 wt%	5	95.0	5.84	94.16	14.0	0.004	17.4	2109 ± 12	560
WC+W 16 wt%	16	84.0	5.14	94.86	16.4	0.002	17.7	2535 ± 07	625

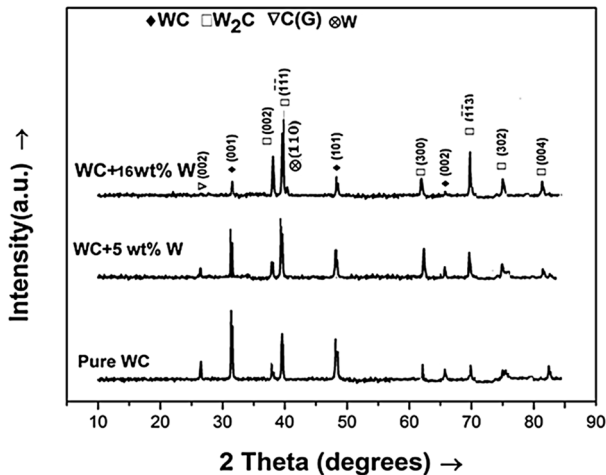


**Fig. 2** XRD patterns observed for arc plasma melt-cast WC+W (0–16 wt%) samples

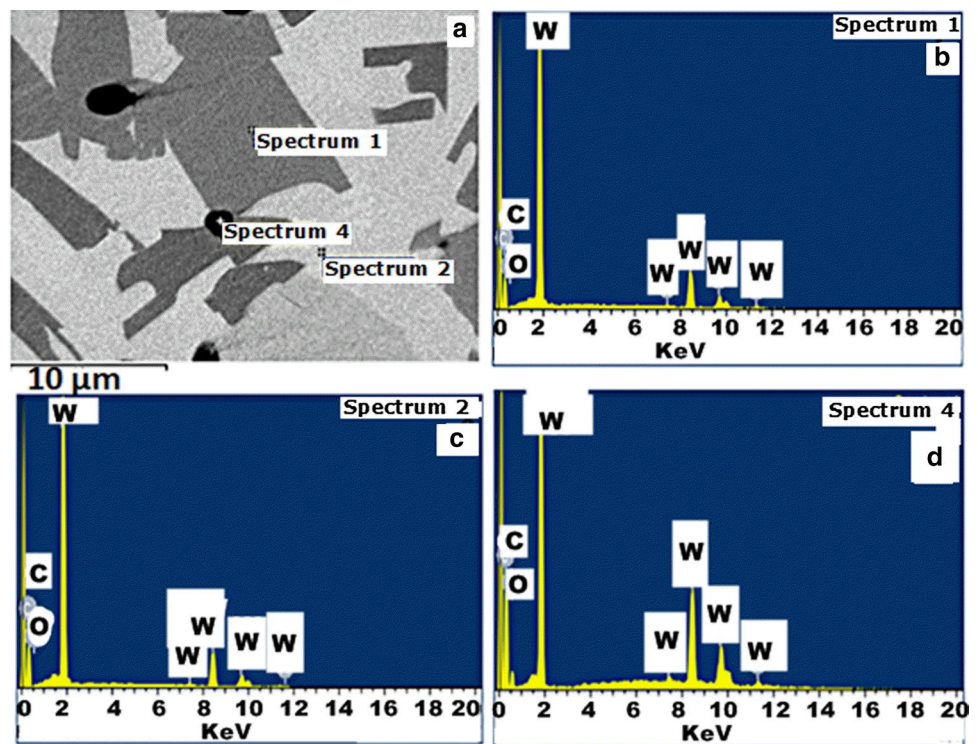
values with JCPDS data files (1999) as follows: WC: 73-0471, W<sub>2</sub>C: 79-0743, C (graphite-2H): 41-1487 and W: 04-0806. In this research work, it is observed that WC, W<sub>2</sub>C and C(G) (graphite) crystallize in hexagonal crystal system. The XRD patterns thus confirmed the composite formation between WC and W<sub>2</sub>C. Basically all melt-cast samples show WC and W<sub>2</sub>C as major phases marked by higher intensity of peak. Melt-cast pure tungsten carbide (WC) sample shows higher intensity peak for WC than W<sub>2</sub>C. It is noticed that the intensity of XRD peaks for W<sub>2</sub>C increases with increasing W wt% in WC matrix. Among the samples, samples with 16 wt% W shows high intense peak of W<sub>2</sub>C phase at around two theta of 38, 39.2 and 69.0 in comparison to other melt-cast products. Whereas WC phase observed at around two theta of 32 and 48.0 show a decreasing trend of intensity.

Dissociation/decomposition reaction was possibly taking place in tungsten carbide at 1250–1300 °C (W<sub>2</sub>C ⇌ (W) + WC [12]) leads to contribute to the presence of W metal (at around two theta of 40 °C) in WC–W<sub>2</sub>C composite. C is marked as small peak in melt-cast pure WC and WC+W (5 wt%) samples due to presence of free C (graphite).

### 3.3 Microstructural studies

FESEM microstructure of typical analysis samples show three phase polycrystalline microstructure in Fig. 3a. Phases/grains/areas such as white, grey and black were observed in microstructure. EDS on these three grains were taken and shown in Fig. 3. Figure 3b–d show EDS taken on grey, white and black areas/grains respectively. The grains shows elements of W and C except black area which additionally has a trace element O. This black area may be due to the presence of pores which % is observed very less in the composite. The intensity of C was found more at black grain/area. Optical, TEM microstructure, EDS and SAED analyses of the melt cast composite samples shown in Fig. 4. Typical grain structures are seen in Fig. 4a–c with EDS shown for the TEM micrograph (Fig. 4d). Optical micrograph for 5 wt% W and 16 wt% W added in WC showed in Fig. 4a and b respectively. Optical micrographs show also three types of grains/areas as it was seen by FESEM. In comparison to WC + 5 wt% W, the WC–W<sub>2</sub>C composite formed from WC + 16 wt% W mixture shows more amount of white grains. In collaborating to XRD and FESEM results, it is observed that white and grey grains may be due to more contribution of W<sub>2</sub>C and WC phases respectively. The microstructure of typical WC–W<sub>2</sub>C composite (W 16 wt%) shown by TEM image also exhibits similarly three types of grains or phases. EDS analysis (Fig. 4d) of typical WC–W<sub>2</sub>C composite (W 16 wt%) composite shows the presence of elements of W, C, O and Cu. The appearance of Cu in the analysis is because of using of Cu coated carbon grid during EDS analysis. Presence of oxygen in trace amount in EDS analysis is due to use of the semi-open type plasma furnace/reactor for melting and casting of composites. No impurity phase is detected in the composite. SAED analysis (Fig. 4e) of typical WC–W<sub>2</sub>C composite (W 16 wt%) sample clearly shows of composite formation between WC and W<sub>2</sub>C after melt-cast of composition. Presence of free C(G) can be corroborated to EDS and XRD results.

**Fig. 3** **a** FESEM micrograph of arc plasma melt-cast WC+W 16 wt%; **b–d** are EDS analysis of arc plasma melt-cast WC+W 16 wt% sample taken on grey, white and black grains/areas respectively



### 3.4 X-ray micro CT

Figure 5a and b show the external (surface) and internal (morpho-structure) images respectively recorded for the melt-cast WC–W<sub>2</sub>C composite (W 16 wt%) sample by employing the non-destructive radiation technique such as X-ray micro CT. Specimen was used in its natural form without processing or preparation like thin sectioning, surface polishing. From the 3D tomographic study, it is found that our melt-cast product is non porous in nature and the sample is free from any type of damages and cracks which supplements our density calculation and TEM analysis results.

### 3.5 FTIR and XPS analyses

FTIR spectrum of WC–W<sub>2</sub>C composite (W 16 wt%) shows (Fig. 6) peaks due to vibrational stretching of W–C in hexagonal crystal structure, C=C (aromatic) stretching and O–H stretching at 1039 cm<sup>-1</sup>, 1634 cm<sup>-1</sup> and 3430 cm<sup>-1</sup> [26, 27] respectively. FTIR analysis further corroborates to our XRD, SAED and EDS results for confirming about the purity of composite without having any presence of impurity. X-ray photoelectron spectra (XPS) were recorded employing AlK $\alpha$  X-ray radiation. The binding energies (B.E.) obtained in W4f and C1s levels of WC–W<sub>2</sub>C composite (W 16 wt%) sample with their peak assignments. The high resolution spectra of W4f state (Fig. 7a) displays two

different bonding states of W. Binding energy values of W4f<sub>7/2</sub> and W4f<sub>5/2</sub> peaks in range of 31.55 eV and 33.9 eV respectively are assigned to both hexagonal phases of WC and W<sub>2</sub>C [12]. Figure 7b shows the de-convoluted high-resolution spectra of C 1s. The complex spectrum of C 1s is de-convoluted into three distinct peaks. The peaks at B.E. values in the range of 282.18 and 284.77 eV are attributed to carbidic C bonded to W phases of WC and W<sub>2</sub>C respectively [24]. The other peak observed at B.E. of 285.78 eV can be related to graphite carbon (*sp*<sup>2</sup> bonded C, denoted as C(G)).

### 3.6 Determination of density, microhardness and Young's modulus values

Since densities of W (19.3 g/cm<sup>3</sup>) and WC (15.8 g/cm<sup>3</sup>) are very high, it was expected that melt-cast solidified composite products will show high range of density. The density of composites was determined by Archimedes' principle. Density of melt cast pure WC, WC+W (5 wt%) and WC+W (16 wt%) composites were found to be 16.5 g/cm<sup>3</sup>, 17.4 g/cm<sup>3</sup> and 17.7 g/cm<sup>3</sup> respectively. It is observed that the melt cast products show density more than 16.5 g/cm<sup>3</sup> which expected to enhance mechanical property of composites. Porosities of the melt-cast products were analysed by BET method and it was found that volumes of the pores were mostly in the range of 0.002–0.005 cm<sup>3</sup>/g. After the confirmation of composite structure of the melt

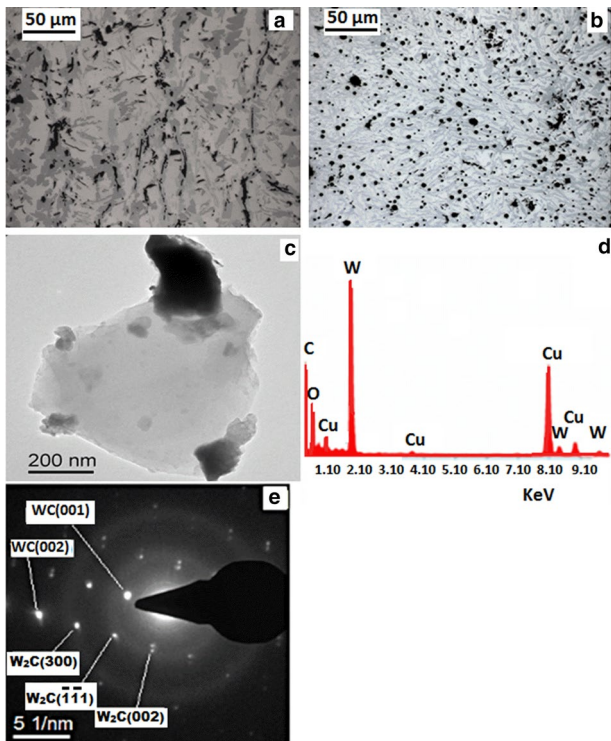


**Fig. 4** Microstructural analysis of arc plasma melt cast sample: **a** and **b** are optical micrographs for WC+W 5 wt% and WC+W 16 wt% respectively; **c–e** are TEM photograph, EDS and SAED pattern for WC+W 16 wt%

cast samples, mirror polished specimens were tested for evaluation of microhardness and Young’s modulus values. It is interesting to note that while pure melt cast WC showed micro hardness at 2020 VHN<sub>0.5</sub>, the rest composite samples showed significant improvements in this value and the highest value at 2535 VHN<sub>0.5</sub> was observed for the WC–W<sub>2</sub>C composite (W 16 wt%) sample prepared by thermal arc plasma technique. While pure melt-cast WC shows Young’s modulus of 510 GPa, WC–W<sub>2</sub>C composite (W 16 wt%) shows Young’s modulus of 625 GPa. WC–W<sub>2</sub>C

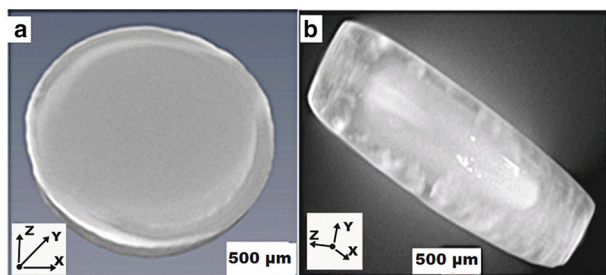


**Fig. 5** X-Ray tomography analysis of melt-cast WC–W<sub>2</sub>C composite (W 16 wt%) sample: **a** surface tomographic image; **b** internal tomographic image

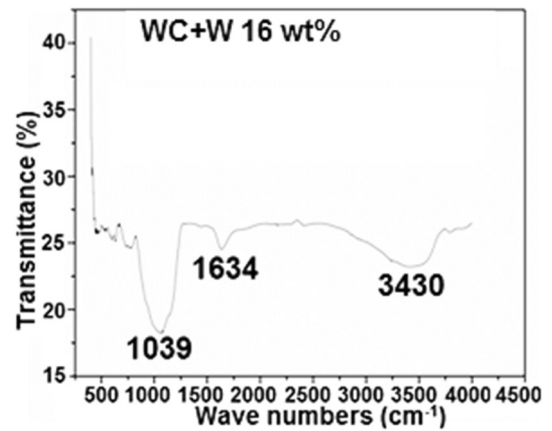


**Fig. 6** FTIR spectra of WC+W 16 wt% sample

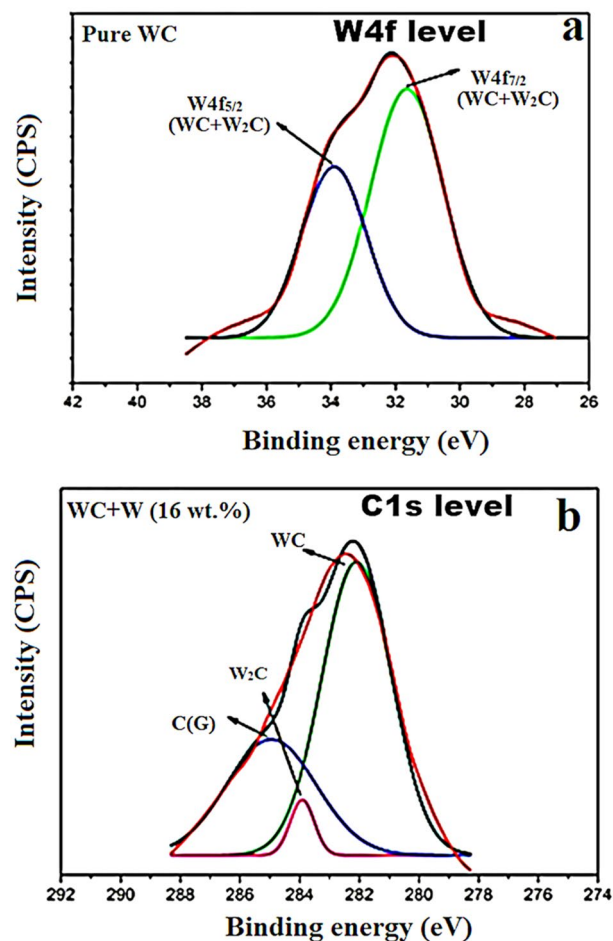


**Fig. 7** XPS spectra of WC+W 16 wt% sample: **a** W4f level and **b** C1s level

composite (16 wt% W) exhibits 25% and 21% relatively higher microhardness and Young’s modulus values than that of pure melt cast WC sample.

The improved microhardness and Young's modulus values of tungsten carbide composites can be attributed to the growth of more amount of  $W_2C$  (higher intensity marked in XRD) phase along with least porosity/pore volume ( $0.002 \text{ cm}^3/\text{g}$ ) and improved density after processing of materials by arc plasma thermal treatment. Hence the WC- $W_2C$  composites prepared by arc plasma melt-cast technique in this work without any metallic binder can be considered as a suitable hard and tough material and can be implemented for various hard facing applications.

## 4 Conclusion

In this work thermal arc plasma melt-cast method has been proved a possible alternate suitable method over conventional methods to prepare successfully three different composites of WC- $W_2C$  from WC + W (0, 5 and 16 wt% W) mixture compositions with improved behavior within 15 min of operation (in dc extended mode). Along with WC and  $W_2C$ , unbound C (graphite) and W (metal) have been found to grow in the composites. WC- $W_2C$  composite formation was confirmed from XRD, EDS, FTIR, XPS and SAED studies. Morpho-structural investigation of typical melt-cast WC- $W_2C$  composite (W 16 wt%) sample by X-ray micro CT reveals the quality of product and the non-existent of the significant pores over the matrix. The melt cast products show high density more than  $16.5 \text{ g}/\text{cm}^3$  which is found higher than that of theoretical value of WC. Pore volume of composites found in the range of  $0.002\text{--}0.005 \text{ cm}^3/\text{g}$ . Polycrystalline type of microstructures was confirmed from microscopic analysis done by optical microscopy, FESEM and TEM. FESEM shows possible presence trace amount of pores. Melt-cast WC- $W_2C$  composite (W 16 wt%) was found to exhibit 25% and 21% significantly higher hardness (2535 VHN) and Young's modulus (625 GPa) values respectively in comparison to that of pure WC with minimal porosity.

## Compliance with ethical standards

**Conflict of interest** On behalf of all authors, the corresponding author states that there is no conflict of interest.

**Open Access** This article is licensed under a Creative Commons Attribution 4.0 International License, which permits use, sharing, adaptation, distribution and reproduction in any medium or format, as long as you give appropriate credit to the original author(s) and the source, provide a link to the Creative Commons licence, and indicate if changes were made. The images or other third party material in this article are included in the article's Creative Commons licence, unless indicated otherwise in a credit line to the material. If material is not included in the article's Creative Commons licence and your intended use is not permitted by statutory regulation or exceeds the permitted

use, you will need to obtain permission directly from the copyright holder. To view a copy of this licence, visit <http://creativecommons.org/licenses/by/4.0/>.

## References

1. Yih SHW, Wang CT (1981) Tungsten sources, metallurgy, properties and applications. Plenum Press, New York
2. Mukhopadhyaya A, Basu B (2011) Recent developments on WC-based bulk composites. *J Mat Sci* 46:571–589
3. Khechba M, Hanini F, Halimi R (2011) Study of structural and mechanical properties of tungsten carbides coatings. *Nat Technol Rev* 05:09–11
4. Oliveira FAC, Granier B, Badie JM, Fernandes JC, Rosa LG, Shohoji N (2007) Synthesis of tungsten sub-carbide  $W_2C$  from graphite/tungsten powder mixtures by eruptive heating in a solar furnace. *Int J Refract Met Hard Mater* 25:351–357
5. Kublii VZ, Velikanova TY (2004) Structural studies of materials-ordering in the carbide  $W_2C$  and phase equilibria in the tungsten-carbon system in the region of its existence. *Powd Metall Met Ceram* 43:630–644
6. Rudy E (1970) Technical report AFML-TR-69-117, Part V, The phase diagram of W-B-C. Wright-Patterson Air Force Base, Ohio, USA, 6
7. Yang ZWuY, Gu D, Li Q, Feng D, Chen Z, Bo Tu, Webley PA, Zhao D (2009) Silica-templated synthesis of ordered mesoporous tungsten carbide/graphitic carbon composites with nanocrystalline walls and high surface areas via a temperature-programmed carburization route. *Small* 23:2738–2749
8. Toth LE (1971) Transition metal carbides and nitrides. Academic Press, New York
9. Jiang G, Zhuang H, Li W (2004) Combustion synthesis of tungsten carbides under electric field I. Field activated combustion synthesis. *Ceram Int* 30:185–190
10. Kim HC, Shon IJ, Yoon JK, Doh JM (2007) Consolidation of ultrafine WC and WC-Co hard materials by pulsed current activated sintering and its mechanical properties. *Int J Refract Met Hard Mater* 25:46–52
11. Almond EA, Roebuck B (1988) Identification of optimum binder phase compositions for improved WC hard metals. *Mater Sci Eng, A* 105(106):237–248
12. Dash T, Nayak BB (2013) Preparation of WC- $W_2C$  composites by arc plasma melting and their characterisation. *Ceram Int* 39:3279–3292
13. Zhou PL, Xiao DH, Zhou PF, Yuan TC (2018) Microstructure and properties of ultrafine grained AlCrFeCoNi/WC cemented carbides. *Ceram Int* 44:17160–17166
14. Ghasali E, Ebadzadeh T, Alizadeh M, Razavi M (2018) Mechanical and microstructural properties of WC-based cermets: a comparative study on the effect of Ni and Mo binder phases. *Ceram Int* 44:2283–2291
15. Kim HC, Shon IJ, Yoon JK, Doh JM, Munir ZA (2006) Rapid sintering of ultrafine WC-Ni cermets. *Int J Refract Met Hard Mater* 24:427–431
16. Wang Z, Jia J, Cao L, Sun N, Wang Y (2019) Microstructure and mechanical properties of spark plasma sintered  $Si_3N_4$ /WC ceramic tools. *Materials* 12(1868):1–11
17. Sandoval DA, Roa JJ, Ther O, Tarrés E, Llanes L (2019) Micromechanical properties of WC-(W, Ti, Ta, Nb)C-Co composites. *J Alloys Compd* 777:593–601
18. Raihanuzzaman RM, Xie Z, Hong SJ, Ghomashchi R (2014) Powder refinement, consolidation and mechanical properties of cemented carbides-an overview. *Powder Technol* 261:1–13

19. Dash T, Nayak BB, Abhangi M, Makwana R, Vala S, Jakhar S, Rao CVS, Basu TK (2016) Preparation and neutronic studies of tungsten carbide composite. *Fusion Sci Technol* 65:241–247
20. Yih SWH, Wang CT (1981) Tungsten sources, metallurgy and applications. Plenum Press, New York
21. Romanova N, Chekulaev P, Dusev V, Lifshitz T, Kurdov M (1972) Sintered metal carbides. Mir Publishers, Moscow
22. Nayak BB (2003) Enhancement in the microhardness of arc plasma melted tungsten carbide. *J Mater Sci* 38:2717–2721
23. Dash T, Nayak BB (2019) Tungsten carbide-titanium carbide composite preparation by arc plasma melting and its characterization. *Ceram Int* 45:4771–4780
24. Dash T, Nayak BB (2016) Preparation of multi-phase composite of tungsten carbide, tungsten boride and carbon by arc plasma melting: characterization of melt-cast product. *Ceram Int* 42:445–459
25. Sahu RK, Mukherjee V, Dash T, Pradhan SK, Biswal SK, Nayak BB (2019) Production of C/SiC nanotubes by arc plasma treatment. *Mater Today Proc* 18:575–581
26. Debalina B, Kamaraj M, Murthy BS, Chakravarthi SR, Sarathi R (2010) Generation and characterization of nano-tungsten carbide particles by wire explosion process. *J Alloys Compd* 496:122–128
27. Yacob AR, Hanapi SZ, Inderan V (2009) Nano tungsten carbide supported on carbon from palm kernel shell in remediation of chlorofluorocarbon (CFC-12). *Int Conf Comput Eng Technol* 185:556–563

**Publisher's Note** Springer Nature remains neutral with regard to jurisdictional claims in published maps and institutional affiliations.